BJUI
BJU INTERNATIONAL

Serenoa repens extract targets mitochondria and activates the intrinsic apoptotic pathway in human prostate cancer cells

Antonella Baron*, Mariangela Mancini*†, Elizabeth Caldwell‡, Anna Cabrelle*, Paolo Bernardi*§ and Francesco Pagano*

**Venetian Institute of Molecular Medicine, †Urological Clinic, and §Department of Biomedical Sciences, University of Padova, Padova, Italy, and ‡Electron Microscopy Laboratory, Fred Hutchinson Cancer Research Center, Seattle, WA, USA*

Accepted for publication 10 September 2008

OBJECTIVE

To investigate the effects of *Serenoa repens* extract (Sr) in human PC3 and LNCaP prostate cancer and MCF7 breast cancer cells, with specific emphasis on the role of the mitochondrial apoptotic pathway, as the molecular pathway through which Sr, a natural product of plant origin, induces death of prostate cancer cells in culture is still unknown.

MATERIAL AND METHODS

Cellular and mitochondrial structure and function, and the cell cycle, were analysed using light, electron and fluorescence microscopy, spectrophotometry and flow cytometry. Apoptosis was evaluated using biochemical and cytohistochemical methods.

RESULTS

Cells treated with Sr underwent massive vacuolization and cytosolic condensation, followed by cell death only in the prostate lines. Within minutes of adding Sr to prostate cells, it caused opening of the permeability transition pore (PTP), which led to complete mitochondrial depolarization within 2 h, and to the appearance of small, pycnotic mitochondria. Release of cytochrome c and SMAC/Diablo to the cytosol was detectable after 4 h of treatment, while caspase 9 activation and poly(ADP-ribose) polymerase 1 cleavage occurred at 16 h, followed by appearance of a sub-G1 peak and apoptosis at 24 h.

CONCLUSION

Sr selectively induces apoptotic cell death of prostate cancer cells through the intrinsic pathway, and activation of the mitochondrial PTP might play a central role in this process.

KEYWORDS

Serenoa repens, Permixon, apoptotic intrinsic pathway, prostate cancer cells, mitochondria

INTRODUCTION

Prostate cancer is the most common malignancy in men, especially in the Western world. Despite considerable progress in its management, predicting the outcome is still extremely difficult for individual patients, given the variable natural history of the disease. The long latency period led to an increasing use of 'complementary' and 'alternative' therapies which might, in part at least, account for the internationally wide variations in the prevalence and mortality of prostate cancer. Asian men who migrate to North America have a greater mortality rate from prostate cancer than men in their native countries [1]. This implies that environmental factors, rather than genetics alone, contribute substantially to the risk of prostate cancer. Experimental and epidemiological studies show that several agents found in the human diet might prevent the effects of carcinogens or suppress the promotion of initiated neoplastic prostatic cells [2].

An extract of the saw palmetto, *Serenoa repens* (Sr) is widely used in the cure of urinary tract ailments and especially for BPH. This phytochemical is prescribed routinely in Europe to relieve the symptoms of BPH, and is the most common herbal remedy used to promote prostate health in the USA. Despite the increasing consideration of urologists for the use of Sr in treating men with symptomatic BPH, its clinical efficacy remains controversial [3,4]. Nonetheless, Sr is one of the most common self-prescribed medications used not only by patients with BPH but also by patients with existing prostate cancer in conjunction with conventional medical treatments. However, no data are available on whether Sr had anti-apoptotic effects that might be exploited for treating prostate cancer in men.

Sr is a complex mixture of saturated and unsaturated fatty acids (FAs), sterols, flavonoids and alcohols [5,6]. Based on the results of *in vitro* and *in vivo* animal and human studies, several mechanisms of action have been proposed for the effects of Sr, including inhibition of 5α-reductase, inhibition of dihydrotestosterone binding to the androgen receptor, anti-inflammatory effects mediated by the inhibition of cyclooxygenase (COX) and lipoxygenase (LOX), and inhibition of fibroblast and epidermal growth factor-induced prostate cell proliferation [7,8]. Sr has also been found to inhibit proliferation and to induce cell death, but the underlying mechanisms are still not completely clarified. While in some studies cell death has been attributed to the

induction of both necrosis and apoptosis, other investigations have discounted apoptosis as a possible mechanism [6,9]. Assessing whether a drug is capable of inducing apoptosis is a highly relevant question for its use as a therapeutic agent.

Given the striking effects of FAs on mitochondria [10], and their potential relevance in causing cell death in prostate cancer cells [11], in the present study we characterized the mitochondrial and cellular effects of Sr, with specific emphasis on prostate epithelial cell growth and the induction of apoptosis through the mitochondrial pathway.

MATERIALS AND METHODS

Human prostate cancer PC3 and LNCaP cells were grown in RPMI 1640, and MCF7 human breast cancer cells were grown in Dulbecco Modified Eagle Medium. Both media were supplemented with 10% fetal calf serum (Life Technologies, Inc., Invitrogen, Paisley, Scotland), 100 U/mL of penicillin, 100 ng/mL of streptomycin, and 2 mM L-glutamine. Tetramethylrhodamine methyl ester (TMRM), 5,5′,6,6′-tetrachloro-1,1′,3,3′-tetraethyl-benzimidazolylcarbocyanine iodide (JC-1), nonyl-acridine-orange and MitoTracker red 580 were obtained from Molecular Probes (Invitrogen). ApopTag™ fluorescein in situ apoptosis detection kit was obtained from Chemicon International (Temecula, CA, USA). Cyclosporin A (CsA) was purchased from Sigma-Aldrich (St Louis, MO, USA), and cyclosporin H (CsH) Alexis Biochemicals (AXXORA, LLC, San Diego, CA, USA). Primary antibodies used were anticytochrome c monoclonal antibody (BD PharMingen, Franklin Lakes, NJ, USA), anti-SMAC-Diablo and monoclonal anti-poly(ADP-ribose) polymerase 1 (PARP) antibodies (Upstate, Lake Placid, NY, USA), anti-Mn superoxide dismutase (Stressgen Biotechnologies, San Diego, CA, USA), and anti-β-actin (Sigma-Aldrich). Enhanced chemiluminescence peroxidase-labelled antirabbit and antimouse antibodies (Amersham Biosciences, Piscataway, NJ, USA) were used as secondary antibodies. Caspase 9 activation was analysed using Caspase 9 FLICA Apoptosis detection kit (Immunochemistry Technologies, LLC, Bloomington, MN, USA). Sr (Permixon®) was provided by Pierre Fabre Médicament, Castres, France. Stock solutions were freshly prepared in dimethyl sulphoxide (DMSO) and diluted in the cell culture to final concentrations as indicated.

To test the effects of Sr on cell viability, cells were plated in 100 mm diameter dishes at a density of 5×10^5 cells/dish, cultured in complete medium to 70% confluency, then treated with 10, 50, 80, 100 μg/mL of Sr or vehicle for the indicated times. Cell viability was assessed using trypan-blue exclusion and propidium iodide (PI) staining. A haemocytometer was used to determine total cell counts.

For electron microscopy, cells were harvested in PBS (in mM, 140 NaCl; 2.7 KCl; 1.5 KH_2PO_4; 8.1 Na_2HPO_4) by gentle scraping and were pelleted by centrifugation. The cell pellets were resuspended in half-strength Karnovsky's fixative for 4–6 h, rinsed in 0.1 M cacodylate buffer, and post-fixed in 1% collidine-buffered osmium tetroxide. Dehydration in graded ethanol and propylene oxide was followed by infiltration and embedding in Epon 812. Sections of 70–90 nm were stained using saturated, aqueous uranyl acetate and lead tartrate. Photographs were taken using a transmission electron microscope (100 SX; Jeol, Ltd, Tokyo, Japan) operating at 80 kV.

To analyse the cell cycle, asynchronous cells (5×10^5/mL) were cultured in the presence of Sr. After incubation, cells were harvested and washed in PBS, fixed in 70% cold ethanol for 60 min at –20 °C, washed in PBS, and incubated for 15 min in PBS containing 100 μg/mL RNase (Sigma) and 50 μg/mL PI (Sigma). In all, 25 000 events per sample were acquired for data analysis using a FACS Calibur (Becton Dickinson, Franklin Lakes, NJ, USA), and the CELLQUEST software to exclude doublets by selective gating. The results were modelled using ModFit (VERITY Software House, Inc., Topsham, ME, USA).

The terminal deoxynucleotidyltransferase-mediated dUTP nick-end labelling (TUNEL) assay was used with the ApopTag Fluorescein *in situ* apoptosis detection kit according to the manufacturers' instructions. Flow cytometric analysis of ApopTag fluorescein- and PI-counterstained cells was used to correlate the DNA content of cell with apoptosis. Briefly, cells were fixed in 1% formaldehyde (pH 7.4) for 15 min on ice, washed twice in PBS, pipetted into 5 mL of 70% ethanol and stored at 20 °C until ready for use. Cells were washed twice in PBS and resuspended in 50 μL of TdT reaction buffer for 30 min at 37 °C, rinsed twice in stop buffer, resuspended in 100 μL of anti-digoxigenin-fluorescein conjugate, incubated 30 min at room temperature, and washed twice with 1 mL of 0.1% Triton X-100 in PBS. At the end of the washing step, DNA counterstaining was carried out by re-suspending the cellular pellets in 1 mL of PBS containing 2.5 μg/mL PI and 10 μg/mL DNase-free Rnase, and incubating them for 30 min at room temperature. Single and double strand-breaks were visualised using fluorescence microscopy of cell suspensions fixed in freshly diluted 1% paraformaldehyde, dried on microscope slides, post-fixed in ethanol:acid acetic (2:1) for 5 min and treated as for FACS analysis. Positive controls were prepared by pre-treating cells with DNase I for 5 min at room temperature. Cells were scored as positive when a green signal was present in the nuclei.

Mitochondrial membrane potential was evaluated with the potentiometric probes JC-1 and TMRM. JC-1 stocks (1 mg/mL in DMSO) were freshly diluted with complete culture medium. Cells were harvested, incubated with medium containing JC-1 (10 μg/mL) for 10 min, washed free of JC-1 and resuspended in 1 mL PBS for flow cytometry analysis. JC-1 shows membrane-potential dependent accumulation in mitochondria, indicated by a shift in its fluorescence emission from green to red due to the formation of JC-1 aggregates [12]. Mitochondrial depolarization is indicated by a decrease in the red/green fluorescence ratio. For fluorescence microscopy with TMRM, cells (50×10^3) were seeded onto round glass coverslips in six-well plates. After the various treatments, cells were washed and incubated in Hanks' balanced salt solution in the presence of 20 nM TMRM and either 1 μM CsH or 1 μM CsA for 30 min at 37 °C. Treatment of control cells with CsH is necessary because the extent of cell and hence mitochondrial loading with potentiometric probes is affected by the activity of the plasma membrane multidrug resistance P-glycoprotein, which is inhibited by both CsH and CsA, whereas only CsA inhibits the permeability transition pore (PTP). Mitochondrial morphology was visualized by confocal microscopy after MitoTracker Red580 staining. Cells plated onto 13 mm diameter round coverslips were cultured to 70% confluency, treated with Sr 100 mg/mL or 1% DMSO for 14 h and labelled with 250 nM MitoTracker Red580 at 37 °C for

*FIG. 1. Effect of Sr on growth and viability of PC3, LNCaP and MCF7 cells. Subconfluent PC3 (panels A, A′), LNCaP (panels B, B′) and MCF7 cells (panels C, C′) were treated with DMSO (open squares) or with 10 (closed circles), 50 (closed squares), 80 (closed triangles) or 100 μg/mL (closed diamonds) of Sr. Panels A- C; at the indicated times cells were counted using a haemocytometer. Panel A′-C′, cell viability was determined on the basis of trypan-blue exclusion assay. Data represent the mean (SD) of three independent experiments. *P = 0.05 compared to untreated.*

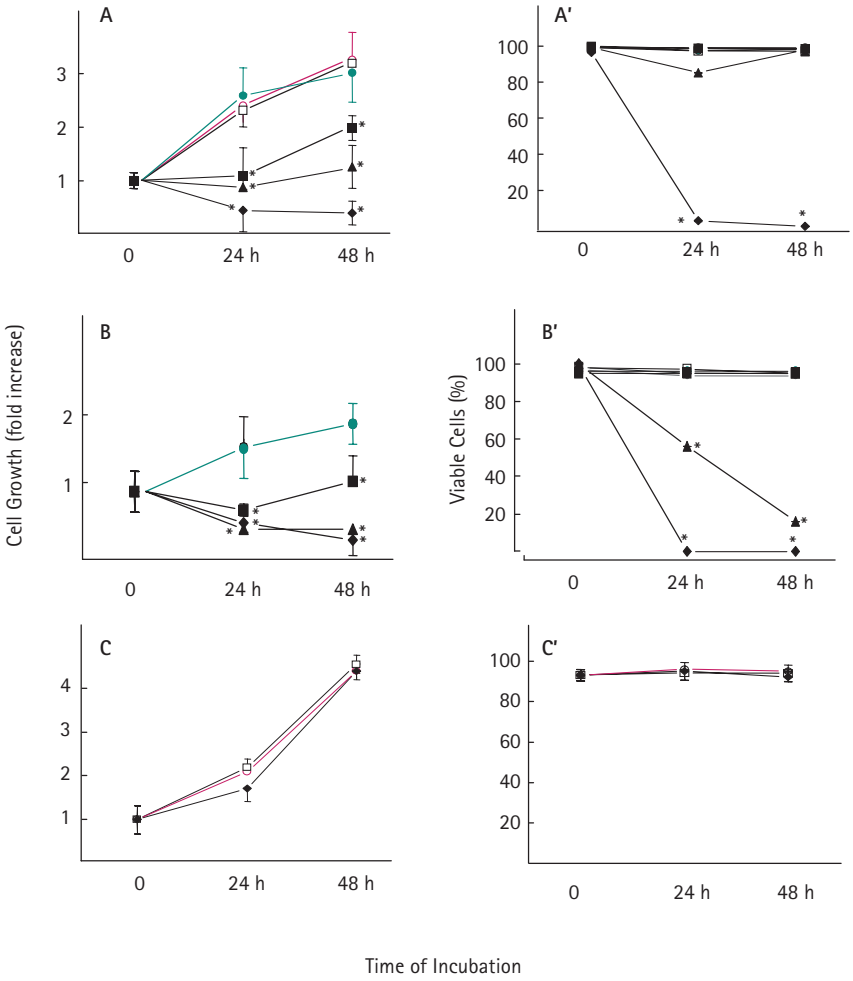

20 min. After two washes with PBS, cells were incubated with medium and visualized under the confocal microscope. Preparation of liver mitochondria, and mitochondrial absorbance changes at 540 nm, which report mitochondrial volume changes, were performed as described previously [13].

Cellular lysates were prepared and immunoblotted as described previously [14]; 50 μg of protein were separated by 10% SDS-PAGE (NuPage, Invitrogen), transferred onto nitrocellulose membranes, and probed using the indicated antibodies conjugated to horseradish peroxidase. Signals were detected using enhanced chemiluminescence (Amersham). Densitometry was performed using a GS170 Calibrated Imaging densitometer, and data were analysed using Quantity One software (Biorad, Hercules, CA, USA).

Caspase 9 activity was detected with the carboxyfluorescein FLICA Apoptosis Detection kit (Immunochemistry Technologies). Briefly, at the designated time points, PC3 cells were rinsed with fresh culture media, replaced with 300 μL/well of 1 × FLICA solution in culture medium, and incubated at 37 °C for 1 h under 5% CO_2. Cells were counterstained with Hoechst dye (0.5% v/v) for 5 min, washed with PBS, and observed through an inverted fluorescent microscope with the appropriate band-pass filter. Non-apoptotic cells appeared unstained, whereas cells undergoing apoptosis fluoresced brightly. Apoptosis was quantified as the percentage of fluorescent cells over 200 cells counted in triplicate.

All experiments were performed in triplicate, and data are reported as the mean (SD) unless otherwise indicated. Comparisons among multiple groups were made using Student's *t*-test and Pearson's chi-square test; 95% CI ($P = 0.05$) were considered to indicate significance.

RESULTS

We assessed the effect of Sr on growth and viability of PC3, LNCaP and MCF7 cells. In PC3 cells Sr at 10 μg/mL had no effect on cell growth at 24 and 48 h, while at 50 and 80 μg/mL it caused growth arrest at 24 h, which was relieved at 48 h, when the cell number increased (Fig. 1A). Cell viability was affected significantly at a dose of 100 μg/mL of Sr, with all cells becoming trypan blue-positive within 24 h (Fig. 1A′). The results were similar in LNCaP cells (Fig. 1B,B′) while Sr had no effects in human breast MCF7 cells (Fig. 1C,C′).

Treatment of cells with 100 μg/mL of Sr induced dramatic morphological changes in PC3 and LNCaP within 4 h, as shown by phase-contrast microscopy, with massive vacuolization and swelling, followed by cytosolic condensation, rounding and detachment of cells from the plate (Fig. 2A); however, MCF7 cells did not become round or detach (Fig. 2A), while vacuolization was apparent, particularly at higher magnification (not shown). The initial swelling of PC3 and LNCaP cells was matched by an increase in cellular size as measured by flow cytometry, while cells treated with doses of Sr of <100 μg/mL still had the initial extensive vacuolization (results not shown) but did not die, as shown by the increase in cell number (Fig. 1A,B).

To gain further insight into the alterations caused by Sr, cells were also analysed by electron microscopy. Using 100 μg/mL of Sr, from early time points up to 24 h of treatment, PC3 cells showed a dramatic derangement of the ultrastructure. In particular, we first detected extensive cytosolic vesiculation and lipid accumulation, followed by cytosolic condensation,

chromatin margination, nuclear pycnosis, cellular fragmentation and formation of apoptotic bodies. At high magnification, the cellular organelles appeared disrupted, a feature particularly evident at the mitochondrial level. At 14 h of treatment, the mitochondria appeared small and pycnotic, with severe matrix condensation, massive swelling of the cristae and signs of membrane disruption (Fig. 2B, panel d). By contrast, at the same time point, cellular chromatin was not yet affected by apoptotic changes (Fig. 2B, panel d, inset). These data indicate that the mitochondrial changes induced by treatment with Sr precede the nuclear changes, suggesting an early involvement of mitochondria in Sr-induced apoptosis. We previously showed this same pattern of pathognomonic early mitochondrial changes preceding the nuclear changes in a similar model of drug-induced apoptosis in colon cancer cells [15].

We next evaluated the nuclear morphology of PC3 cells treated with Sr and stained with PI. Within 24 h of exposure to 100 μg/mL of Sr, half the cells had chromatin condensation and nuclear fragmentation (Fig. 3A). Cell-cycle analysis showed the presence of a sub-G1 peak (corresponding to cells containing fragmented DNA) in 8.9% of the population at 24 h, which increased to 18.3% at 48 h of treatment. These changes were matched by a decrease in the G0/G1 peak (13% and 23% at 24 and 48 h, respectively) and an accumulation of cells in G2/M phase (2.4% and 3.2% at 24 and 48 h, respectively; Fig. 3B and Table 1).

As described above (Fig. 1A) in PC3 cells, Sr at doses of ≤80 μg/mL induced growth arrest at 24 h. This state corresponds to an increase of cells in the G0/G1 phase and a parallel decrease of cells in the S phase. The cells in the S phase decreased by 3.5%, 7.5% and 9.3% at 10, 50 and 80 μg/mL, respectively. The growth arrest was overcome at 48 h when cell-cycle phases were distributed as in the control (Table 1). The behaviour at 100 μg/mL was similar in LNCaP cells, while Sr had no effects on the distribution of MCF7 cells through the cell cycle (Table 1).

We also simultaneously measured DNA content (cell cycle) and apoptotic strand breaks (DNA fluorescein-dUTP labelling) in cells treated with 100 μg/mL Sr. TdT labelling was detectable by flow cytometric analysis after 14 h of treatment (data not shown) and involved 35% and 70% of the cell population at 24 and 48 h, respectively (Fig. 3C). TdT labelling was not confined to a specific phase of the cell cycle (Fig. 3C, panel a). TdT labelling was also visualised by fluorescence microscopy in immunostained cells counterstained with PI. Positive cells showed green fluorescent spots,

FIG. 2. Effect of Sr on PC3 cell morphology, size and ultrastructure. Panel A, Light microscopy images (×400) of PC3, LNCaP and MCF7 cells treated with 100 μg/mL Sr for 4 h (centre), 24 h (right) or with vehicle (left). Panel B, Electron microscopy images of PC3 cells treated with vehicle (panels a, c) or with Sr 100 μg/mL for 24 h (panel b) or 14 h (panel d). Magnification is indicated on each panel. Note that changes in mitochondrial ultrastructure, such as condensation and pycnosis, swelling of the cristae and membrane fragmentation (panel d, arrow and arrowhead, respectively) are evident before detectable changes in nuclear and chromatin morphology (inset to panel d).

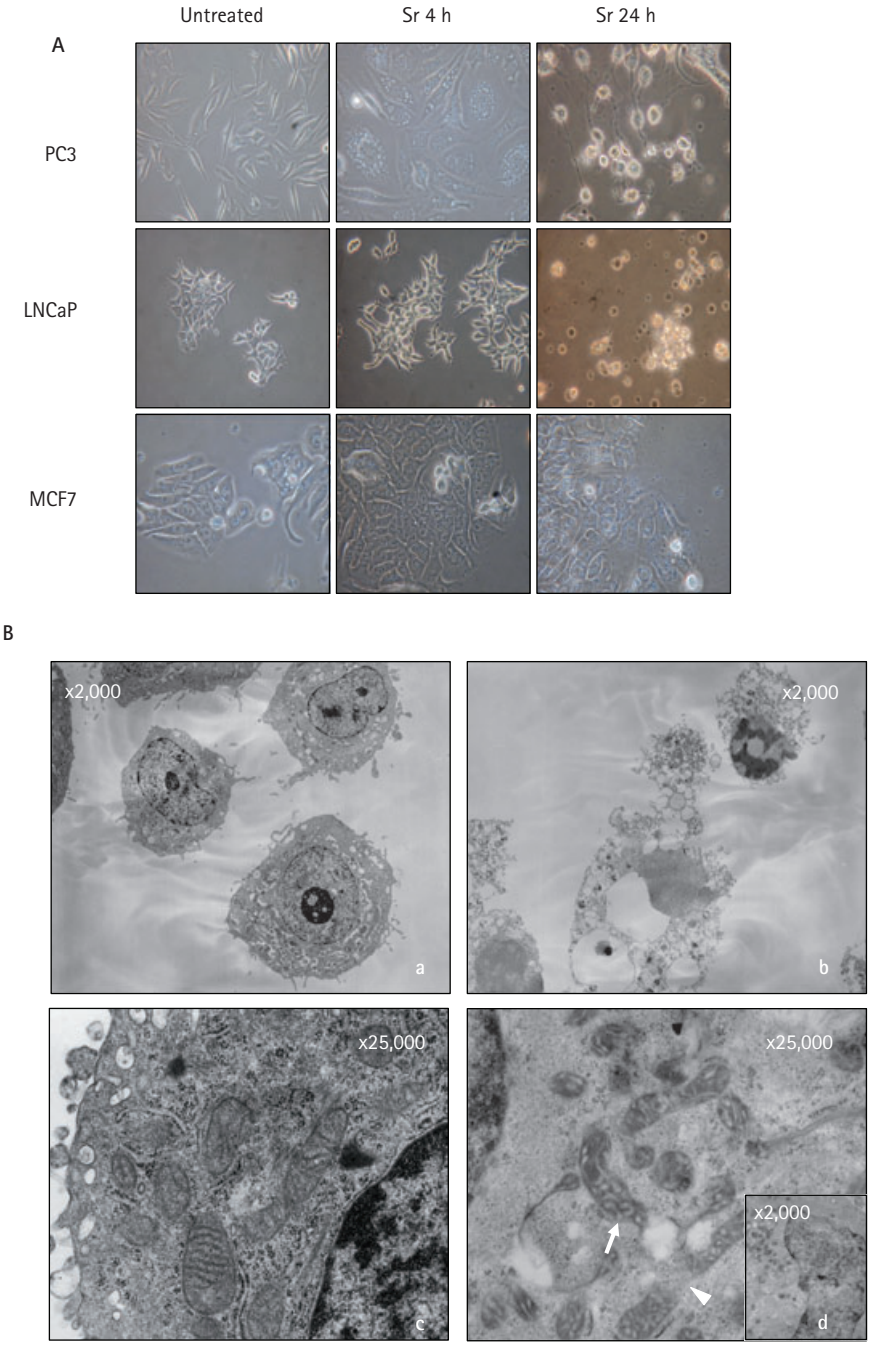

FIG. 3. Apoptotic effect of Sr on PC3 cells. Panel A, PC3 cells were fixed with 70% ethanol and stained with PI 24 h after treatment with vehicle (a) or with Sr 100 μg/mL (b), and nuclear morphology was assessed by fluorescence microscopy. Apoptotic nuclei (b, arrows) were detected in about half the Sr-treated cells (c). Panel B, cell-cycle distribution of PC3 cells treated with Sr. The DNA content of PC3 cells treated with the indicated doses of Sr was analysed by flow cytometry at 24 and 48 h. A sub-G1 peak (light blue) characteristic of apoptosis was present in 100 μg/mL Sr-treated cells at 24 and at 48 h. Panel C, TdT flow cytometry analysis of PC3 cells treated with 100 μg/mL Sr for 24 h. The plots (a) report the DNA content on the x-axis and TdT-labelled apoptotic DNA strand breaks on the y-axis. At 24 and 48 h, 35% and 70% of cells were TdT-positive, with all cell-cycle phases equally involved. Note that the population with increased TdT-labelling, which is shifted above the baseline, was equally distributed through all cell-cycle phases. TdT uptake was also analysed by fluorescence microscopy, and nuclei were counterstained with PI (b). The positive apoptotic cells show green fluorescence.

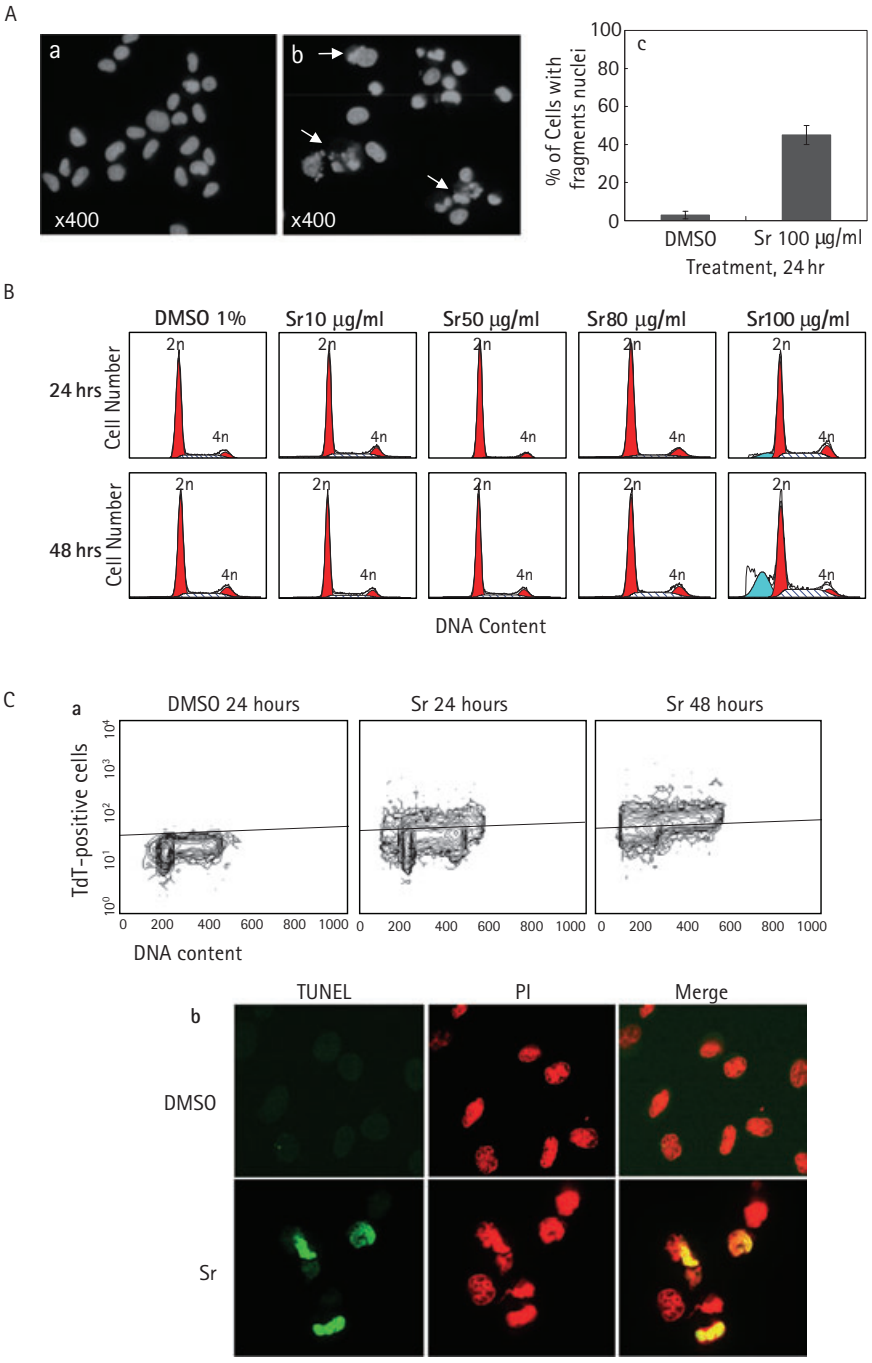

corresponding to the presence of single- and double-stranded DNA breaks in the red PI counterstained nuclei (Fig. 3C, panels b). Taken together, the results of the cell-cycle analysis suggest the involvement of an apoptotic process in the death of Sr-treated cells.

We evaluated the effects of Sr treatment on the morphology and membrane potential of mitochondria. Mitochondrial morphology was visualized by *in situ* staining with MitoTracker Red580. Analysis by confocal microscopy showed that mitochondria of PC3 cells changed shape dramatically, from reticular-elongated to punctated-fragmented within 14 h of exposure to Sr, a change that involved mitochondria in the vast majority of treated cells (Fig. 4A). To evaluate the effects of Sr treatment on mitochondrial function we determined the *in situ* mitochondrial membrane potential based on the accumulation of the potentiometric probes JC-1 and TMRM.

JC-1 in its monomeric form emits green fluorescence. Upon accumulation in mitochondria in response to the mitochondrial membrane potential the dye forms multimers, which emit red fluorescence. Although signal calibration is only possible in isolated mitochondria, these emission properties allow monitoring of the mitochondrial membrane potential *in situ*, where a decreased mitochondrial transmembrane potential causes a decrease in the red fluorescence and an increase of the green fluorescence. Treatment with Sr caused a dramatic decrease in the red/green fluorescence ratio that could be detected as early as 2 and 12 h of treatment with 100 μg/mL Sr in PC3 and LNCaP cells, respectively, but not in MCF7 cells (Fig. 4B). TMRM is a rhodamine-based cationic lipophilic probe that accumulates in energized mitochondria *in situ*. When used at concentrations below the mitochondrial quenching threshold, mitochondrial depolarization is indicated by a decrease in mitochondrial fluorescence (i.e. TMRM release from the matrix) [16]. Treatment of PC3 cells with 100 μg/mL Sr caused complete release of mitochondrial TMRM within 2 h (Fig. 4C). These experiments indicated that mitochondrial depolarization is an early consequence of treatment of PC3 cells with Sr, suggesting that Sr might initiate cell death through the intrinsic, mitochondrial pathway.

TABLE 1 The effect of Sr on cell distribution through the cell cycle

Cell line and Sr dose, μg/mL	% at 24 h				% at 48 h			
	Sub G1	G0/G1	S	G2/M	Sub G1	G0/G1	S	G2/M
PC3								
Control	0.6	65.0	15.8	18.5	0.8	69.4	14.2	15.6
10	0.8	73.5	12.3	13.4	1.0	68.3	15.8	14.9
50	0.6	80.2*	8.3*	10.9	0.9	71.6	13.6	13.9
80	0.9	78.8*	6.5*	13.8	0.9	68.1	13.6	17.4
100	8.9*	52.0	18.2	20.9	18.3*	46.4*	16.5	18.8
LNCaP								
Control	0.3	74.2	11.2	10.3	1.4	89.7	1.8	3.8
100	6.5	36.5*	24.0*	33.0*	9.61*	40.2*	24.0*	22.7*
MCF7								
Control	0.3	67	16	16	1.0	76	14	9
100	0.5	61	23	16	0.8	74	14	11

*SubG1, G0/G1, S and G2/M populations were determined as described in Materials and Methods, and quantified using the ModFit software program. Results are expressed as the percentage of cells in each phase of the cell cycle. *denotes statistically significant differences vs 1% DMSO-treated control cells.*

We tested whether Sr caused a release of mitochondrial apoptogenic proteins. Cytochrome c was released within 4 h of treatment, and the amount detected in the cytosolic fraction increased further at 6 h, together with SMAC/Diablo (Fig. 5A). Within the same period Mn-superoxide dismutase was only detectable in the mitochondrial fraction, indicating that the release of the intermembrane apoptogenic proteins was selective rather than due to disruption of mitochondria (Fig. 5A). Release of mitochondrial proteins does not necessarily lead to apoptosis. We therefore tested the status of apical caspase-9 and of downstream targets of effector caspases. PC3 cells treated with Sr had a clear increase in caspase-9 activity (Fig. 5B). Furthermore, the 85 kDa fragment of PARP produced by the action of activated caspase-3 was detected, with a clear decrease in full-length PARP at 16 h of incubation (Fig. 5C).

FAs are powerful inducers of the PTP in isolated mitochondria and in intact cells [10,11,17,18]. As opening of the PTP causes activation of the mitochondrial apoptosis pathway in several models [18,19], we tested the effects of Sr on the absorbance of a mitochondrial suspension at 540 nm, a reliable method to detect mitochondrial volume changes due to PTP opening [13]. After adding a small Ca^{2+} pulse that was not sufficient to trigger PTP opening per se (not shown), adding 100 μg/mL Sr caused a process that can be ascribed to PTP opening, because it was inhibited by CsA, which desensitizes the PTP to the inducing effects of Ca^{2+} and inorganic phosphate [20] (Fig. 6A). Remarkably, adding 100 μg/mL of Sr to PC3 cells caused a rapid process of mitochondrial depolarization which could be prevented by treatment with CsA (Fig. 6B).

DISCUSSION

In the present study we showed that a well-characterized extract of Sr causes growth arrest and apoptosis of prostate cancer PC3 cells. The features were similar in LNCaP prostate cancer cells but not in MCF7 breast cancer cells, confirming that the effects of Sr are specific for prostate-derived cell lines [21]. After some debate, the vast majority of studies agree that Sr causes apoptosis [22–28]. The remarkable new finding of the present study is that apoptosis depends on the intrinsic pathway, which appears to be triggered by opening of the mitochondrial PTP, a high-conductance channel that is involved in many forms of cell death [20]. Our results provide a solid mechanistic basis for the pro-apoptotic effects of Sr. As PC3 cells do not express androgen receptors, these findings also suggest that Sr might be beneficial for the treatment of hormone-resistant prostate cancer.

Despite its widespread use, there is controversy about whether Sr is clinically beneficial in BPH and in other urological disorders [4,29]. As the active principle(s) components underlying the biological responses to Sr remain undefined, the discrepancies might largely depend on the use of different commercial products in which these components could vary substantially. In the present study we used a well-characterized preparation approved for clinical use. Although the composition of the Sr is complex, we think that identifying mitochondria as targets offers useful insights into the active components.

Permixon is a mixture largely composed of free FAs, which comprise up to 90% of the preparation. The most relevant are oleic acid (C18:1, 36.0%), lauric acid (C12:0, 27.5%), myristic acid (C14:0, 12.0%) and palmitic acid (C16:0, 9.7%). Esterified FAs represent 7%, while the remainder is composed of phytosterols and polyprenic compounds [5]. The mitochondrial effects of free FAs are extremely well characterized, and might provide a 'reading frame' for the pro-apoptotic effects of Sr.

After forming thioesters with CoA, FAs are excellent respiratory substrates in most types of cells. However, free FAs can also interact with mitochondrial membranes and increase their permeability. In particular, they can: (i) increase proton conductance of the inner membrane, causing dissipation of the electrochemical proton gradient and

FIG. 4. Effect of Sr on mitochondrial morphology and membrane potential in PC3 cells. Panel A, confocal microscopy images of PC3 cells stained with MitoTracker Red580 before (left) and after 14 h of treatment with 100 μg/mL Sr (centre). After treatment the mitochondria assumed a rounded punctate morphology in 83% of treated cells (right). Panel B, representative examples of flow cytometry analysis of the mitochondrial membrane potential after JC-1 staining of PC3 (top row), LNCaP (middle row) or MCF7 cells (bottom row). ND, not done. The mitochondrial potential decreased sharply starting 2 and 12 h after treatment with 100 μg/mL Sr, as shown by the decrease in the red fluorescence, in PC3 and LNCaP cells, respectively, while it had no effects in MCF7 cells. Panel C, representative images of analysis of the mitochondrial membrane potential in PC3 cells by fluorescence microscopy with TMRM 2 h after treatment with vehicle (ethanol, left) or Sr (right).

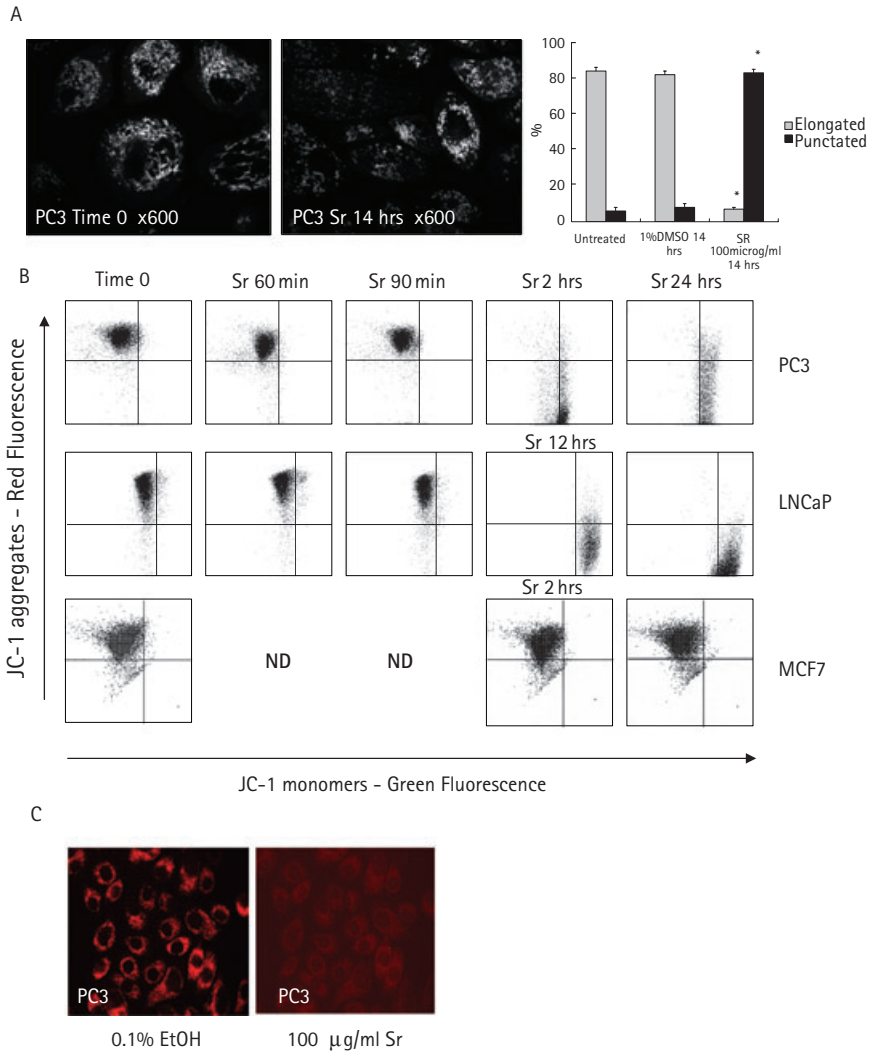

therefore decreasing ATP synthesis; and (ii) promote opening of the PTP with depolarization, loss of ionic homeostasis, matrix swelling, outer membrane rupture and release of apoptogenic proteins [10]. Thus, free FAs are dual effectors with the potential to improve energy production (as substrates) or to cause energy dissipation (as uncoupling agents and modulators of ion channels).

Previous studies indicated that both saturated and unsaturated C14, C16 and C18 FAs are effective at inducing swelling and uncoupling in isolated mitochondria [17]. On the other hand, the FA features necessary to cause depolarization of mitochondria *in situ* and cytotoxicity depend on the cell type. In a hepatoma cell line the presence of double bonds was required, the minimum number of unsaturations needed to observe the effects increasing with the length of the hydrocarbon chain [17]. In other cell types, prominent mitochondrial effects and/or cytotoxicity were also shown by a saturated FA like palmitic acid, a relevant component of Sr [10]. These findings raise the interesting possibility that the mitochondrial pro-apoptotic effects of Sr are mediated, in part at least, by its contents of FA.

An important open question is the basis for the selectivity of Sr for the prostate [21], which has been confirmed in the present work. Polyunsaturated FAs can enter metabolic pathways without activation to their CoA esters, and the most important for the prostate is arachidonic acid (AA). Prostate cells, which usually maintain very low levels of free AA due to the high activity of COX and LOX, may be particularly sensitive to the killing effects of FA as shown in PC3 cells exposed to very low levels of exogenous AA after pharmacological inhibition of COX and LOX [11]. It appears possible that the uptake of Sr overloads cells with FA that cannot be readily disposed of, causing an increased probability of PTP opening and eventually apoptosis. Studies to verify this hypothesis are currently in progress in our laboratory.

Phytochemicals are extremely promising candidates for the therapy of specific forms of cancer, because they are relatively nontoxic, inexpensive and available for oral administration [30]. No treatment is currently available for hormone-resistant prostate cancer. As Sr selectively induces the death of prostate cancer cell lines through mitochondria, we hope that the results of the present study will encourage further research on the scientific basis for the prostate-specific mitochondrial effects of Sr, and that they might pave the way for a rational treatment of prostate cancer.

ACKNOWLEDGEMENTS

This work was supported by grants from Zegna Foundation (Treviso-Italy) on prostate cancer research to F. Pagano and AIRC to P. Bernardi.

CONFLICT OF INTEREST

None declared.

FIG. 5. Effects of Sr on mitochondrial release of apoptogenic proteins, caspase 9 and PARP activation. Panel A, PC3 cells were treated with 100 μg/mL Sr; at the indicated times mitochondrial and cytosolic fractions were prepared, separated by SDS-PAGE and immunoblotted with the indicated antibodies as described in Methods. Panel B, representative images of caspase 9 activation after 14 h of Sr treatment. Panel C, immunoblot analysis of the time course of PARP activation after treatment of PC3 cells with 100 μg/mL Sr; note the appearance of cleaved PARP after 4 h of treatment.

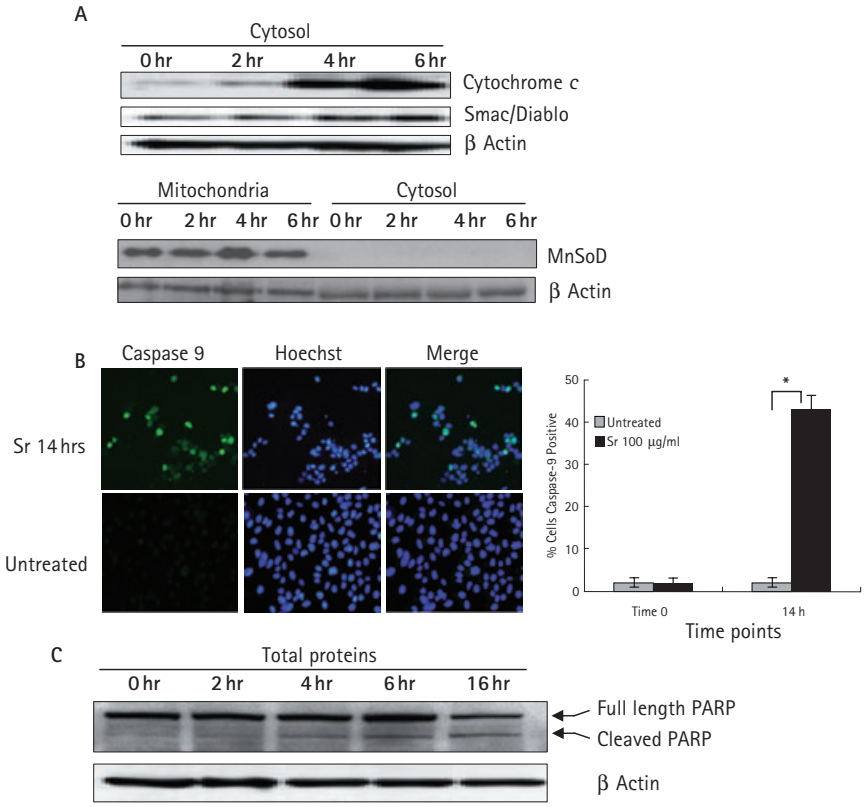

FIG. 6. Sr induces the mitochondrial permeability transition in isolated mitochondria and intact cells. Panel A, liver mitochondria from Albino Wistar rats (0.5 mg/mL) were incubated in 0.25 M sucrose, 10 mM Tris-Mops pH 7.4, 5 mM glutamate-Tris, 5 mM malate-Tris, 1 mM Pi-Tris, 10 μM EGTA-Tris (final volume 2 mL, pH 7.4) in a magnetically stirred cuvette thermostatted at 25 °C, and absorbance measured at 540 nm. Where indicated (arrows) 40 μM Ca^{2+} and 100 μg/mL Sr were added. In the experiment denoted by the dashed trace the incubation medium was supplemented with 0.85 μM CsA. Panel B, PC3 cells on a coverslip were loaded with 10 nM TMRM in the presence of CsA (open symbols) or of CsH (closed symbols) and studied by fluorescence microscopy. Where indicated by the arrows, 100 μg/mL Sr and 2 μM the protonophore carbonylcyanide-p-trifluoromethoxyphenyl hydrazone were added.

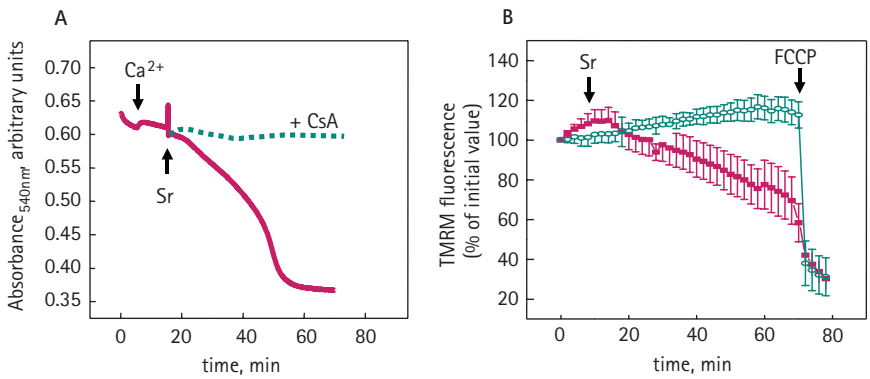

REFERENCES

1 **Shimizu H, Ross RK, Bernstein L, Yatani R, Henderson BE, Mack TM.** Cancers of the prostate and breast among Japanese and white immigrants in Los Angeles County. *Br J Cancer* 1991; **63**: 963–6

2 **Fleshner N, Zlotta AR.** Prostate cancer prevention: past, present, and future. *Cancer* 2007; **110**: 1889–99

3 **Gerber GS, Fitzpatrick JM.** The role of a lipido-sterolic extract of *Serenoa repens* in the management of lower urinary tract symptoms associated with benign prostatic hyperplasia. *BJU Int* 2004; **94**: 338–44

4 **Bent S, Kane C, Shinohara K *et al.*** Saw palmetto for benign prostatic hyperplasia. *N Engl J Med* 2006; **354**: 557–66

5 **Buck AC.** Is there a scientific basis for the therapeutic effects of *Serenoa repens* in benign prostatic hyperplasia? Mechanisms of action. *J Urol* 2004; **172**: 1792–9

6 **Iguchi K, Okumura N, Usui S, Sajiki H, Hirota K, Hirano K.** Myristoleic acid, a cytotoxic component in the extract from *Serenoa repens*, induces apoptosis and necrosis in human prostatic LNCaP cells. *Prostate* 2001; **47**: 59–65

7 **Gerber GS.** Saw palmetto for the treatment of men with lower urinary tract symptoms. *J Urol* 2000; **163**: 1408–12

8 **Goldmann WH, Sharma AL, Currier SJ, Johnston PD, Rana A, Sharma CP.** Saw palmetto berry extract inhibits cell growth and Cox-2 expression in prostatic cancer cells. *Cell Biol Int* 2001; **25**: 1117–24

9 **Hill B, Kyprianou N.** Effect of permixon on human prostate cell growth: lack of apoptotic action. *Prostate* 2004; **61**: 73–80

10 **Bernardi P, Penzo D, Wojtczak L.** Mitochondrial energy dissipation by fatty acids. Mechanisms and implications for cell death. *Vitam Horm* 2002; **65**: 97–126

11 **Gugliucci A, Ranzato L, Scorrano L *et al.*** Mitochondria are direct targets of the lipoxygenase inhibitor MK886. A strategy for cell killing by combined treatment with MK886 and cyclooxygenase inhibitors. *J Biol Chem* 2002; **277**: 31789–95

12 **Reers M, Smith TW, Chen LB.** J-aggregate formation of a carbocyanine as a quantitative fluorescent indicator of membrane potential. *Biochemistry* 1991; **30**: 4480–6

13 **Petronilli V, Cola C, Massari S, Colonna R, Bernardi P.** Physiological effectors modify voltage sensing by the cyclosporin A-sensitive permeability transition pore of mitochondria. *J Biol Chem* 1993; **268**: 21939–45
14 **Seewaldt VL, Caldwell LE, Johnson BS, Swisshelm K, Collins SJ, Tsai S.** Inhibition of retinoic acid receptor function in normal human mammary epithelial cells results in increased cellular proliferation and inhibits the formation of a polarized epithelium in vitro. *Exp Cell Res* 1997; **236**: 16–28
15 **Mancini M, Anderson BO, Caldwell E, Sedghinasab M, Paty PB, Hockenbery DM.** Mitochondrial proliferation and paradoxical membrane depolarization during terminal differentiation and apoptosis in a human colon carcinoma cell line. *J Cell Biol* 1997; **138**: 449–69
16 **Bernardi P, Scorrano L, Colonna R, Petronilli V, Di Lisa F.** Mitochondria and cell death. Mechanistic aspects and methodological issues. *Eur J Biochem* 1999; **264**: 687–701
17 **Penzo D, Tagliapietra C, Colonna R, Petronilli V, Bernardi P.** Effects of fatty acids on mitochondria: implications for cell death. *Biochim Biophys Acta* 2002; **1555**: 160–5
18 **Penzo D, Petronilli V, Angelin A *et al.*** Arachidonic acid released by phospholipase A (2) activation triggers Ca (2+) -dependent apoptosis through the mitochondrial pathway. *J Biol Chem* 2004; **279**: 25219–25
19 **Irwin WA, Bergamin N, Sabatelli P *et al.*** Mitochondrial dysfunction and apoptosis in myopathic mice with collagen VI deficiency. *Nat Genet* 2003; **35**: 367–71
20 **Bernardi P, Krauskopf A, Basso E *et al.*** The mitochondrial permeability transition from in vitro artifact to disease target. *FEBS J* 2006; **273**: 2077–99
21 **Bayne CW, Ross M, Donnelly F, Habib FK.** The selectivity and specificity of the actions of the lipido-sterolic extract of *Serenoa repens* (Permixon) on the prostate. *J Urol* 2000; **164**: 876–81
22 **Hostanska K, Suter A, Melzer J, Saller R.** Evaluation of cell death caused by an ethanolic extract of Serenoae repentis fructus (Prostasan) on human carcinoma cell lines. *Anticancer Res* 2007; **27**: 873–81
23 **Vela-Navarrete R, Escribano-Burgos M, Farre AL, Garcia-Cardoso J, Manzarbeitia F, Carrasco C.** *Serenoa repens* treatment modifies bax/bcl-2 index expression and caspase-3 activity in prostatic tissue from patients with benign prostatic hyperplasia. *J Urol* 2005; **173**: 507–10
24 **Wadsworth TL, Worstell TR, Greenberg NM, Roselli CE.** Effects of dietary saw palmetto on the prostate of transgenic adenocarcinoma of the mouse prostate model (TRAMP). *Prostate* 2007; **67**: 661–73
25 **Vacherot F, Azzouz M, Gil-Diez-De-Medina S *et al.*** Induction of apoptosis and inhibition of cell proliferation by the lipido-sterolic extract of *Serenoa repens* (LSESr, Permixon in benign prostatic hyperplasia. *Prostate* 2000; **45**: 259–66
26 **Yang Y, Ikezoe T, Zheng Z, Taguchi H, Koeffler HP, Zhu WG.** Saw Palmetto induces growth arrest and apoptosis of androgen-dependent prostate cancer LNCaP cells via inactivation of STAT 3 and androgen receptor signaling. *Int J Oncol* 2007; **31**: 593–600
27 **Wadsworth TL, Carroll JM, Mallinson RA, Roberts CT Jr, Roselli CE.** Saw palmetto extract suppresses insulin-like growth factor-I signaling and induces stress-activated protein kinase/c-Jun N-terminal kinase phosphorylation in human prostate epithelial cells. *Endocrinology* 2004; **145**: 3205–14
28 **Hsieh TC, Wu JM.** Mechanism of action of herbal supplement. PC-SPES: elucidation of effects of individual herbs of PC-SPES on proliferation and prostate specific gene expression in androgen-dependent LNCaP cells. *Int J Oncol* 2002; **20**: 583–8
29 **Boyle P, Robertson C, Lowe F, Roehrborn C.** Updated meta-analysis of clinical trials of *Serenoa repens* extract in the treatment of symptomatic benign prostatic hyperplasia. *BJU Int* 2004; **93**: 751–6
30 **Kwon KB, Park BH, Ryu DG.** Chemotherapy through mitochondrial apoptosis using nutritional supplements and herbs: a brief overview. *J Bioenerg Biomembr* 2007; **39**: 31–4

Correspondence: Paolo Bernardi, Department of Biomedical Sciences, Viale Giuseppe Colombo 3, I-35121 Padova, Italy.
e-mail: paolo.bernardi@unipd.it
and
Francesco Pagano, Venetian Institute of Molecular Medicine, Viale Giuseppe Colombo 3, Via Orus 2, I-35129 Padova, Italy.
e-mail: francesco.pagano@unipd.it

Abbreviations: **Sr**, *Serenoa repens* extract; **FA**, fatty acid; **COX**, cyclooxygenase; **LOX**, lipoxygenase; **TMRM**, tetramethylrhodamine methyl ester; **JC-1**, 5,5′,6,6′-tetrachloro-1,1′,3,3′-tetraethyl-benzimidazolylcarbocyanine iodide; **CS**, cyclosporin; **PARP**, poly(ADP-ribose) polymerase 1; **DMSO**, dimethyl sulphoxide; **PI**, propidium iodide; **TUNEL**, terminal deoxynucleotidyltransferase-mediated dUTP nick-end labelling; **PTP**, permeability transition pore; **AA**, arachidonic acid.